Multiple Coloumb Scattering in MicroBooNE

David Kaleko*[1], Polina Abratenko[2], Mike Shaevitz[1], Josh Spitz[2], Leonidas Kalousis[3], and XXX NOTE AUTHOR LIST IS PRELIMINARY, THIS WILL BE A COLLABORATION PAPER XXX[3]

[1]Columbia University, NY
[2]University of Michigan, MI
[3]Misc

November 19, 2016

Abstract

Liquid Argon Time Projection Chambers (LArTPCs) are an important detector technology for the future of the neutrino physics community. This technology allows for, among other things, precise three-dimensional reconstruction of charged particle tracks that traverse the detector medium. The MicroBooNE experiment is a LArTPC at the Fermi National Accelerator laboratory with active volume dimensions of 2.3 m width $\times$ 2.6 m height $\times$ 10.4 m length located in the Booster Neutrino Beamline (BNB) which has a peak neutrino momentum of about 0.7 GeV. In this note, we discuss a technique of measuring a track-like particle's momentum by means of multiple coloumb scattering (MCS), which does not require the full track to be contained inside of the detector volume as other track momentum reconstruction methods do (E.G. range-based momentum reconstruction and calorimetric momentum reconstruction). In this note we provide motivation for why this technique is important, demonstrate and quantify its performance on simulated single tracks, and then demonstrate its performance on fully contained neutrino-induced muon tracks both in simulation and in data. In general we find good agreement between data and simulation, with negligible bias in the momentum reconstruction and with resolutions that vary as a function of track length, between 5% for the longest tracks (several meters long) and 15% for the shortest (one meter long) when 10 centimeter segments are used in the MCS algorithm. This technote also describes other uses for multiple coloumb scattering besides momentum reconstruction, including identification of poorly reconstructed tracks, determination of track direction, and some particle identification capabilities.

*Corresponding Author

Contents

1 Note Content Overview

This is a technote internal to the MicroBooNE collaboration quantifying the performance of the multiple coloumb scattering based momentum estimation technique. While the note may seem lengthy, do not fear. Many sections are essentially the same, containing the same plots constructed in the same way, but from different input samples. In general the structure of this note is as follows:

1. An introduction to the MicroBooNE detector, and motivation for the multiple coloumb scattering method for this experiment and within the future LArTPC community.
2. A detailed description of how the actual method works.
3. Demonstration of this method on single muon MCTracks. The purpose of this is to demonstrate that the technique works with the least obfuscated input.
4. Demonstration of this method on a high-statistics sample of truth-selected muons from well reconstructed simulated numu charged-current interactions. The purpose of this is to demonstrate that the technique works with automatically reconstructed tracks, and its performance is quantified on a relevant sample (where the muons have the momentum and angle spectra that one would expect in MicroBooNE from the BNB). This section also describes optimizing the segment length used in the algorithm, optimizing the additional constant resolution term used in the algorithm, as well as a potential additional use for the technique involving determining track directionality.
5. Demonstration of this method on automatically-selected well-reconstructed neutrino events in the full MicroBooNE BNB + cosmics simulation. The purpose of this section is to get one step towards working with real automatically-selected BNB data. This section describes MID rates, MCS PID capabilities, and other things that the previous (truth-based selection) section does not.
6. Demonstration of this method on automatically-selected real neutrino events in actual MicroBooNE BNB data. In order to ensure the tracks are well-reconstructed and to mitigate MIDs, a handscanning effort is used and is described in this section.
7. A conclusion section reiterating the usefulness of the tool, along with a list of plots that might be good to put in a potential publication derived from this note.

2 Introduction and Motivation

MicroBooNE (Micro Booster Neutrino Experiment) is an experiment based at the Fermi National Accelerator Laboratory (Fermilab) that uses a large Liquid Argon Time Projection Chamber (LArTPC) to investigate the excess of low energy events observed by the MiniBooNE experiment [4] and to study neutrino-argon cross-sections. MicroBooNE is part of the Short-Baseline Neutrino (SBN) physics program, along with two other LArTPCs: the Short Baseline Near Detector (SBND) and the Imaging Cosmic And Rare Underground Signal (ICARUS) detector. MicroBooNE also provides important research and development in terms of detector technology and event reconstruction techniques for future LArTPC experiments includine DUNE (Deep Underground Neutrino Experiment).

The MicroBooNE detector is currently the largest LArTPC in the United States. It consists of a rectangular time projection chamber (TPC) with dimensions 2.3 m width $\times$ 2.6 m height $\times$ 10.4 m height located 470 m away from the Booster Neutrino Beam (BNB) target. Time projection chambers, filled with a gas or liquid volume, are used to analyze particle interactions in three dimensions. The

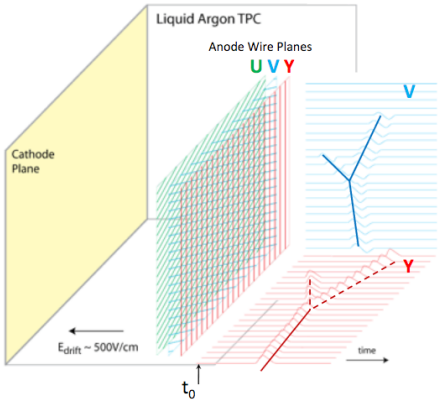

Figure 1: *A diagram of the time projection chamber of the MicroBooNE detector [5].*

x-direction of the TPC corresponds to the drift coordinate, the y-direction is the vertical direction, and the z-direction is the direction along the beam. The amount of active liquid argon in the TPC is 86 tons, with the total cryostat containing 170 tons of liquid argon. Liquid argon is chosen to fill the volume for a variety of reasons: argon contains a high number of nucleons, which allows for a greater rate of interactions with particles within the medium; argon ionizes easily; it produces scintillation light which is not reabsorbed; it has a high electron lifetime; and it is inexpensive.

Photomultiplier tubes (PMTs) and three wire planes with 3mm spacing at angles of 0, and $\pm$ 60 degrees with respect to the vertical are located in the TPC to aid with event reconstruction (Figure 1). In a neutrino interaction, a neutrino from the beam interacts with the argon and the charged outgoing child particles traverse the medium, losing energy and leaving an ionizing trail. The resulting electrons drift to the anode side of the TPC, containing the wire planes, away from the negatively charged cathode plate on the opposite side. The movement of electrons induces a current in the wires, which is used to create three distinct two-dimensional views of the event. Combining these wire signals with timing information from the PMTs allows for full three-dimensional reconstruction of the event.

The BNB is predominantly composed of muon neutrinos, which can undergo charge-current interactions in the TPC and produce muons. For muon tracks that are completely contained in the TPC, it is straightforward to calculate the momentum with a measurement of the length of the particle's track. Around half of muons from BNB neutrino events in MicroBooNE are not fully contained in the TPC, and therefore using length-based calculations for these uncontained tracks is not a possibility. The only way to compute the energy of an outgoing three-dimensional track is by means of multiple coloumb sccattering (MCS).

The phenomenon of multiple coulomb scattering (MCS) occurs when a charged particle enters a medium and undergoes electromagnetic scattering with the atoms. This scattering deviates the original trajectory of the particle within the material (Figure 2). For a given energy, the scatters of a track-like particle form a gaussian distribution centered at zero with a and standard deviation given by the

Highland formula [7]:

$$\sigma_\theta^0 = \frac{13.6 \text{ MeV}}{p\beta c} z \sqrt{\frac{\ell}{X_0}} \Big[1 + 0.0038 \ln\Big(\frac{\ell}{X_0}\Big)\Big] \tag{1}$$

where β is the ratio of the particle's velocity to the speed of light, ℓ is the distance traveled inside the material, and X_0 is the radiation length of the target material (taken to be a constant 14 cm in liquid argon). With the Highland formula, the momentum of a track-like particle can be determined using only the 3D reconstructed track it produces in the detector, without any calorimetric information. The method by which this is done is described in detail in Section 3.

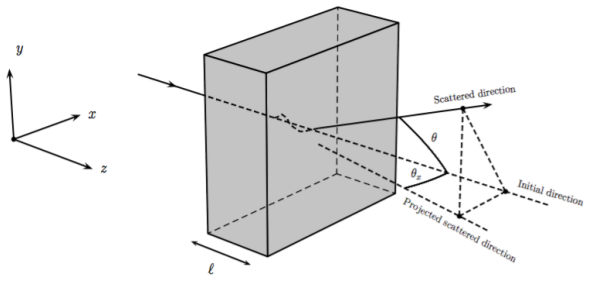

Figure 2: *The particle's trajectory is deflected as it traverses through the material [6].*

3 MCS Implementation Using the Maximum Likelihood Method

This section describes exactly how the phenomenon of multiple coloumb scattering is leveraged to determine the momentum of a track-like particle reconstructed in a LArTPC. In general, the approach is as follows:

1. The three-dimensional track is broken up into segments of configurable length.
2. The scattering angles between each consecutive segment are measured.
3. Those angles combined with the Highland formula (Equation 2) are used to build a likelihood that the particle has a specific momentum, taking into account energy loss in upstream segments of the track.
4. The momentum corresponding to the maximum likelihood is chosen to be the MCS computed momentum.

Each of these steps are discussed in detail in the following subsections.

The idea and initial implementation of MCS using the maximum likelihood method for this analysis is credited to Leonidas Kalousis, a former member of the MicroBooNE collaboration. Further details regarding the technique can be found in his internal notes concerning both Monte Carlo simulated tracks [6] and reconstructed tracks [8]. Only slight modifications to this code have been made for the analysis described in this note.

For this analysis, a minimum start-to-end reconstructed track length of 100 cm was used.

3.1 Track Segmentation

The input to the track segmentation routine is a vector of ordered three-dimensional trajectory points (x,y,z) representing the reconstructed track. The points are ordered along the direction of the track, with the first point representing the start of the track, and the last point representing the end of the track. These trajectory points can be determined in a number of ways by different track reconstruction algorithms. In general, a three-dimensional track is reconstructed by combining two-dimensional hits reconstructed from signals on the different wire planes along with timing information from the photomultiplier tubes to reconstruct the third dimension. In the case of this note, the PandoraNuPMA algorithm is used to reconstruct the track [2].

Also input to the track segmentation routine is the desired segment length, which is a tunable parameter. In this note, segment lengths are generally taken to be 10 cm (based on the findings of Section 5.5) except where otherwise explicitly stated (as in Section 5.5). This routine begins at the start of the track, and iterates through the trajectory points in order, each time computing the straight-line distance between the first point and the current one. When a point is reached that is greater than the desired segment length, that iteration stops and the direction cosines of this segment are computed.

Given the subset of the three-dimensional trajectory points (x, y, z) that correspond to one "segment" of the track, a three-dimensional linear fit is applied to the data points using the orthogonal distance

regression method around the trajectory point averages for that segment. This method finds the eigenvalues and eigenvectors of the (data - average) covariance matrix and the solution is the one associated with the maximum eigenvalue.

At the end of this routine, a vector of length n (where n is the number of segments for the track) is stored containing the direction cosines at the start of each segment.

3.2 Scattering Angle Computation

This routine within the MCS code takes as input the vector of length n (where n is the number of segments for the track) containing the direction cosines at the start of each segment. In general, the algorithm iterates over consecutive pairs of segments (the segmentation routine is described in Section 3.1) and computes angular scatters between each, and stores them for later use by a future subroutine. This code is more complicated than just taking the dot product between consecutive direction cosines to find the total angular scatter between segments because the Highland formula is derived from scattering independently in the two directions orthogonal to the direction of the track. For this reason, this subroutine performs a coordinate transformation for each pair of segments such that the "z" direction (which, in detector coordinates is just the beam direction) is rotated to be along the direction of the first two segments. With the "z" direction as such, "x" and "y" directions are chosen such that all of "x", "y", and "z" are mutually orthogonal. Note that at this point, all of "x", "y", and "z" are different than the similarly named detector coordinates. The scattering angle both in the "x" and "y" planes are then computed for each consecutive pairs of segments. After this routine, a vector of length $2n$ is stored containing the scattering angles in the "x" plane as well as in the "y" plane. These scattering angles are what are input into the maximum likelihood routine to determine track momentum.

3.3 Maximum Likelihood Theory

The normal probability distribution for a variable with a gaussian error sigma is given by:

$$f_X(\Delta\theta_j) = (2\pi\sigma_0^2)^{-\frac{1}{2}} exp(-\frac{1}{2}\frac{(\Delta\theta_j - \mu_0)^2}{\sigma_0^2}) \tag{2}$$

Here, each $\Delta\theta_j$ corresponds to a $\Delta\theta$ measurement between one pair of segments in a track either in the rotated-coordinates "x" or "y" plane, μ_0 is assumed to be zero, and σ_θ^0 is the RMS angular deflection computed by the modified Highland formula (Equation 6), which is a function of both the momentum and the length of that segment. Since energy is lost between segments, σ_θ^0 is different for each angular measurement along the track so we replace σ_θ^0 with σ_θ^j, where j is an index representative of the segment.

To get the likelihood, one takes the product of $f_X(\Delta\theta_j)$ over all the $\Delta\theta_j$ segment-to-segment scatters along the track. Since the product of exponentials is just an exponential with the sum of the arguments, this product becomes

$$L(\mu; (\sigma_\theta^1)^2, ..., (\sigma_\theta^n)^2; \Delta\theta_1, ..., \Delta\theta_n) = \prod_{j=1}^{n} f_X(\Delta\theta_j, \mu, (\sigma_\theta^j)^2) = (2\pi)^{\frac{-n}{2}} \times \prod_{j=1}^{n} (\sigma_\theta^j)^{-1} \times exp(-\frac{1}{2}\sum_{j=1}^{n}\frac{(\Delta\theta_j - \mu_0)^2}{(\sigma_\theta^j)^2}) \tag{3}$$

In practice, rather than maximizing likelihood it is often more computationally convenient to instead minimize the negative log likelihood. Taking the natural logarithm of the likelihood L gives an expression

that is related to a χ^2

$$l(\mu;(\sigma_\theta^1)^2,...,(\sigma_\theta^n)^2;\Delta\theta_1,...,\Delta\theta_n) = ln(L) = -\frac{n}{2}ln(2\pi) - \sum_{j=1}^{n} ln(\sigma_\theta^j) - \frac{1}{2}\sum_{j=1}^{n}\frac{(\Delta\theta_j-\mu)^2}{(\sigma_\theta^j)^2} \tag{4}$$

The negative log likelihood for one specific segment's angular scatter $\Delta\theta_j$ given an expected scattering RMS σ_θ^j is given by the following equation

$$-l(\mu,\sigma_\theta^j,\Delta\theta_j) = \frac{1}{2}ln(2\pi) + ln(\sigma_\theta^j) + \frac{1}{2}\frac{(\Delta\theta_j-\mu)^2}{(\sigma_\theta^j)^2} \tag{5}$$

In general, Equation 5 is evaluated for each segment in a track given a postulated full track momentum, and the sum of these terms is used to determine the likelihood that the postulated track momentum is correct for that track.

3.4 Maximum Likelihood Implementation

Given a set of angular deflections in the "x" and "y" planes for each segment as described in Section 3.2, a modified version of the Highland formula (Equation 6) is used along with a maximum likelihood method to determine the momentum of the track.

$$\sigma_\theta^{RMS} = \sqrt{(\sigma_\theta^0)^2 + (\sigma_\theta^{res})^2} = \sqrt{(\frac{13.6\text{ MeV}}{p\beta c}z\sqrt{\frac{\ell}{X_0}}\Big[1+0.0038\ln\Big(\frac{\ell}{X_0}\Big)\Big])^2 + (\sigma_\theta^{res})^2} \tag{6}$$

where the formula is "modified" from the original Highland formula (Equation 2) in that it includes a detector-inherent angular resolution term σ_θ^{res} which is given a fixed value of 2 mrad in this analysis as described in Section 5.6[8].

In general, this routine does a raster scan over postulated track energies in steps of 1 MeV from a minimum of the full track range-based momentum up to a maximum of 7.5 GeV. Starting with the range-based momentum as a minimum is valid because the range-based momentum is known to be an accurate predictor of momentum for contained tracks (see Section 4.3.3) and is therefore an acceptable minimum both for contained and for exiting tracks. Ending at 7.5 GeV as a maximum momentum is valid because given the BNB spectrum, no neutrino-induced tracks above that momentum are expected in MicroBooNE.

Given a postulated full track momentum, the full track energy E_t is computed from the usual energy momentum relation,

$$E^2 = p^2 + m^2 \tag{7}$$

and the maximum likelihood algorithm iterates over angular scatters for each segment, with two $\Delta\theta_j$ values for each segment (corresponding to the "x" and "y" scattering planes). The energy of the jth segment is given by

$$E_j = E_t - k_{cal} * N_{upstream} * l_{seg} \tag{8}$$

where k_{cal} is the minimally ionizing energy constant given to be $2.105\frac{MeV}{cm}$ in liquid argon[3], $N_{upstream}$ is the number of segments upstream of this particular segment, and l_{seg} is the segmentation length. This definition of E_j therefore takes into account energy loss along the track, and can never be negative given the range of possible E_t values described previously. This value of segment energy is used to predict the

RMS angular scatter for that segment (σ_θ^{RMS}) by way of a modified version of the modified Highland formula, Equation 6. Still assuming the mean angular scatter, μ, is zero, Equation 5 is evaluated for each segment and all evaluations are summed to compute a total summed negative log likelihood for that postulated track energy, E_t.

After the raster scan over postulated track momenta is complete, the one with the smallest summed negative log likelihood is chosen to be the final MCS computed momentum for the track.

4 MCS Performance on Simulated Single Muons

In this section, MCS performance is studied on a sample of simulated, fully contained, single muons in MicroBooNE. This section of the technote will include studies from this single muon sample with MCTracks (described in Section 4.3.1).

It is demonstrated that the range-based momentum of a track agrees with the true momentum with negligible bias and with a resolution of better than 5%. The MCS performance on single MCTracks is shown to be comparable to that on single reconstructed PandoraNuPMA tracks when the track is well reconstructed, with a minimal bias and a resolution that varies between 3 and 13%, performing better for higher momentum (longer) tracks. Additionally, the scattering angle of track segments for a given momentum is shown to be gaussian for MCTracks, in line with the Highland formula prediction.

4.1 Input Sample

In order to study MCS performance in the most straightforward way, a sample of simulated single muons is used. This sample was generated in the MicroBooNE MCC7 production under the SAM definition "prod_muminus_0-2.0GeV_isotropic_uboone_mcc7_reco2". This sample consists of 19,500 single muons generated at a random location within the MicroBooNE TPC, with random direction. The energy spectrum of this sample is flat between 0 to 2 GeV kinetic energy of the muons. It is worth noting that the MCC7 simulation includes broken wires by masking specific channels on some planes in an attempt to better match real detector conditions, however MCTracks are unaffected by this (Section 4.3.1).

4.2 Fiducial Volume Definition

The MicroBooNE TPC has active volume dimensions of 2.3 m width × 2.6 m height × 10.4 m length. For this analysis, a smaller "fiducial volume" is defined and referenced throughout this note (for example, in many cases reconstructed tracks are required to be fully contained within the fiducial volume). For reference, the fiducial volume definition used throughout this note is the full TPC volume reduced in by 20 cm from both the cathode plane and the anode wire planes, shifted in 26.5 cm in from both the top and bottom walls of the TPC, shifted in 20 cm from the beam-upstream wall of the TPC, and shifted in 36.8 cm from the downstream wall of the TPC. The reason for this choice of fiducial volume is that it reduces contamination from "edge effects" that occur near the walls of the TPC, like electric field distortions and space-charge effects. While the TPC has a total active volume of 62.6 m^3, the fiducial volume used in this analysis has a volume of 38.7 m^3 or roughly 62% of the total TPC active volume.

4.3 Performance with MCTracks

4.3.1 MCTrack Description

MCTrack objects are made from the output of geant4, and are created from geant4 energy depositions in the detector. geant4 outputs 3D energy depositions in the detector, along with truth information about which parent particles deposited this energy. MCTracks are 3D objects which are formed by grouping the energy depositions based on parent particles. Whether a particle in geant4 is turned into an MCTrack or an MCShower (not discussed in this note) is based on truth PDG (for example,

muons, protons, and pions always form MCTracks).

Each MCTrack is itself a vector of 3D trajectory points, which are ordered to match the direction of the particle that deposited the energy. Trajectory points are only formed for energy depositions inside of the TPC volume. In general, long MCTracks will have steps separated by up to several centimeters. Each step in an MCTrack holds the following information used in this analysis: 3D position, and true energy at that point. Only information within the realm of reconstructable quantities is used in this analysis, with the exception of true energy (which is used for example to quantify a reconstructed energy resolution).

Since the output of a nominal reconstruction chain (going through hit finding, clustering, matching across planes, etc.) are 3D tracks, MCTracks can be studied in an analysis in the exact same way as a reconstructed track would be. MCTracks can be thought of as perfectly reconstructed tracks, where each trajectory point along the track is a true 3D energy deposition inside of the MicroBooNE TPC.

Since MCTracks are formed from true 3D energy depositions and not from wire signals on drift electrons, MCTracks are insensitive to broken wires, noise, and other simulated detector effects.

4.3.2 MCTrack Selection

For analysis on single muon MCTracks, the input sample is the one described in Section 4.1. From that sample, the following requirements are placed for event selection:

1. There is exactly one MCTrack in the event.
2. The MCTrack is longer than one meter in start-to-end length.
3. The MCTrack is fully contained within the fiducial volume (defined in Section 4.2).
4. The MCTrack does not decay in flight.

After these selection requirements are placed, the intial sample of 19,500 muons is reduced to 623 which are used for analysis.

4.3.3 Range Momentum Validation

With this sample of MCTracks, it is possible to quantify MCS momentum resolution as a function of true momentum. However, in actual MicroBooNE data there is obviously no true momentum with which to compare. The additional momentum handle that is used in data for contained tracks is range-based momentum. The stopping power of muons in liquid argon is well described by the particle data group[1]. By using a linear interpolation between points in the cited PDG stopping power table, the start-to-end straight-line length of a track can be used to reconstruct the muon's total momentum with good accuracy. Figure 3 shows a comparison of range momentum to true momentum for this sample.

In order to compute a bias and a resolution, Figure 3 is sliced in bins of true muon energy and a histogram of the fractional energy difference ($\frac{E_{range}-E_{true}}{E_{true}}$) is created for each bin. This distribution is shown for three representative bins in Figure 4. The mean of each distribution is used to compute a bias as function of true energy, while the standard deviation of each distribution is used to compute a resolution. Figure 5 shows the bias and resolution for the range-based energy reconstruction method. It can be seen that the bias is negligible and the resolution for this method of energy reconstruction

is on the order of 2-4%. Based on this figure, it is clear that range-based energy (and therefore range-based momentum) is a good handle on the true energy (momentum) of a reconstructed muon track in MicroBooNE data, assuming that track starts and ends near the true start and end of the muon.

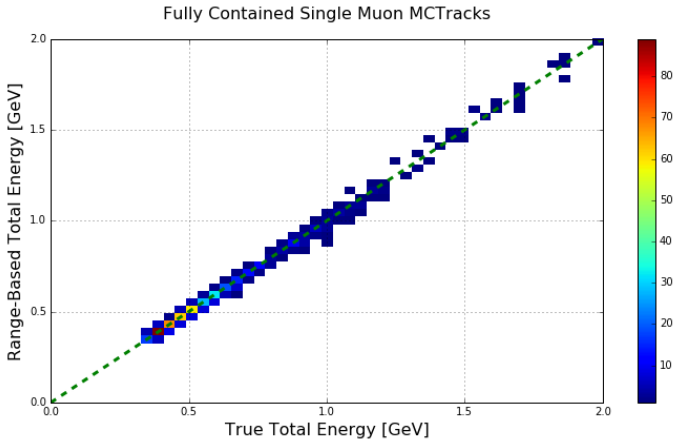

Figure 3: *Range based energy versus true energy for the single muon* MCTrack *sample described in Section 4.3.2.*

4.3.4 MCS Momentum Validation

For this sample of MCTracks, only the 3D trajectory points of each MCTrack are used as input to the MCS code, described in Section 3. The resulting MCS momentum versus range-based momentum can be seen in Figure 6. Range momentum is used here instead of true momentum in order to make this plot more directly comparable with the same analysis on data where true momentum is not accessible. In order to compute a bias and a resolution, Figure 6 is sliced in bins of range momentum and a histogram of the fractional momentum difference ($\frac{p_{MCS}-p_{range}}{p_{range}}$) is created for each bin. This distribution is shown for three representative bins in Figure 7. The mean of each distribution is used to compute a bias a

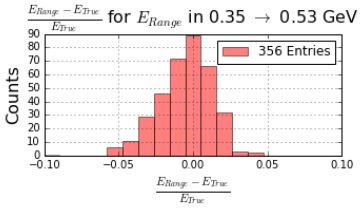

(a) *Fractional energy difference between 0.35 and 0.53 GeV true energy.*

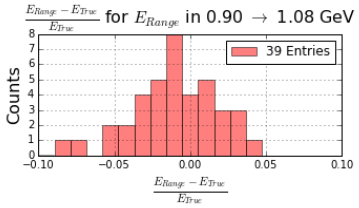

(b) *Fractional energy difference between 0.90 and 1.08 GeV true energy.*

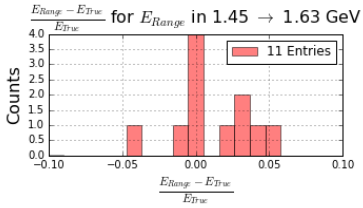

(c) *Fractional energy difference between 1.45 and 1.63 GeV true energy.*

Figure 4: *Fractional energy difference for a few representative bins of true energy derived from Figure 3.*

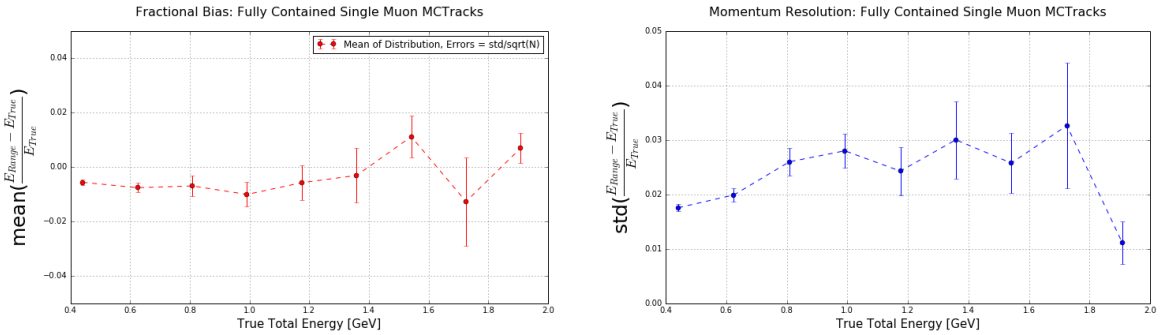

(a) *Range energy bias as a function of true energy.* (b) *Range energy resolution as a function of true energy.*

Figure 5: *Range energy and true energy bias and resolution for the single muon* MCTrack *sample described in Section 4.3.2.*

function of range momentum, while the standard deviation of each distribution is used to compute a resolution. The bias and resolution for this momentum reconstruction method shown in Figure 8. This figure indicates a bias in the MCS momentum resolution on the order of a few percent, with a resolution that decreases from about 12% for contained MCTracks with true total momentum around 0.5 GeV (which corresponds to a length of about 1.7 meters) to below 6% for contained MCTracks with true total momentum greater than 0.8 GeV (which corresponds to a length of about 3.1 meters).

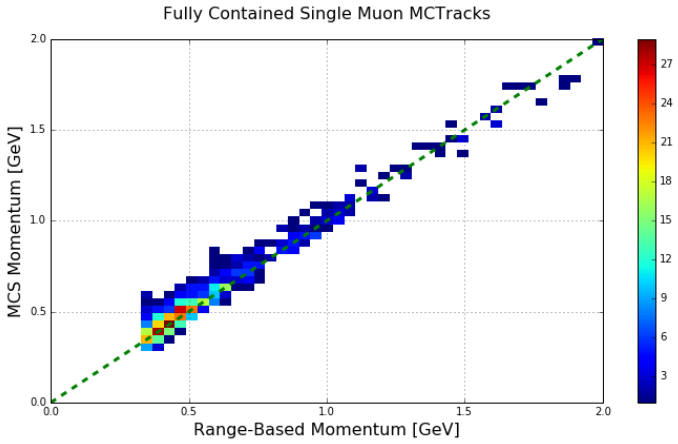

Figure 6: *MCS computed momentum versus range momentum for the single muon* MCTrack *sample described in Section 4.3.2.*

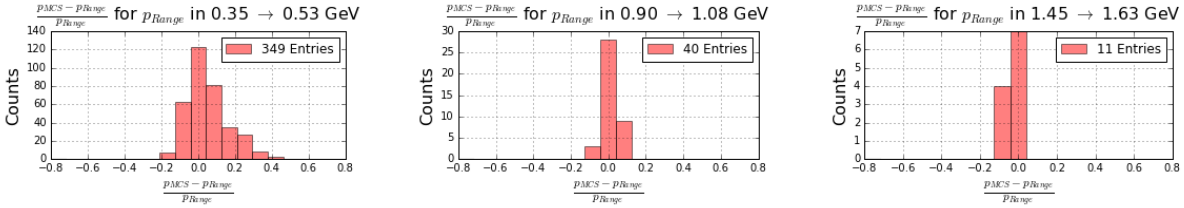

(a) *Fractional momentum difference between 0.35 and 0.53 GeV range momentum.*

(b) *Fractional momentum difference between 0.90 and 1.08 GeV true momentum.*

(c) *Fractional momentum difference between 1.45 and 1.63 GeV true momentum.*

Figure 7: *Fractional momentum difference for a few representative bins of range momentum derived from Figure 6.*

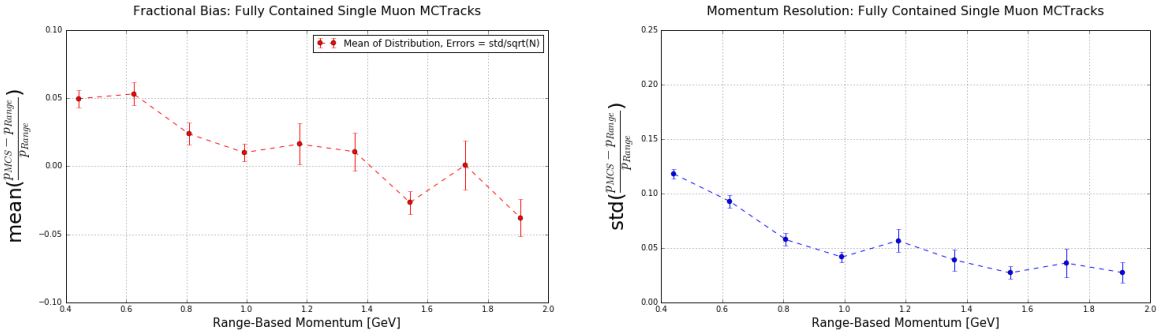

(a) *MCS momentum bias as a function of range momentum.*

(b) *MCS momentum resolution as a function of range momentum.*

Figure 8: *MCS momentum bias and resolution as a function of range momentum for the single muon* MCTrack *sample described in Section 4.3.2.*

4.3.5 Highland Validation

For a given track segment momentum and length, 98% of the angular scatter deviations should be gaussian with an RMS described by the Highland equation (Equation 2), while the remaining 2% are larger angle Rutherford scatters[7] [XXX note this citation might be wrong, paper is behind a paywall right now, need to double check]. Therefore, a histogram of track segment angular deviations divided by the RMS predicted by the Highland equation should be gaussian with a width of unity. In this section, we validate this claim.

For each 10 cm segment of each MCTrack in this single muon sample, the momentum of the muon at the start of that segment is estimated by taking the computed MCS momentum and subtracting out momentum lost in the track upstream of the start of this segment, assuming the track was minimally ionizing as described in Equation 8. The segment momentum, along with the segment length, is converted into an expected RMS angular deviation by way of Equation 2. For each consecutive pair of segments, the angular scatter in milliradians divided by the Highland expected RMS in millradians is an entry in the histogram shown in Figure 9. From this figure we can see that the Highland formula is valid for MCTracks, as the gaussian fit agrees well with the underlying histogram.

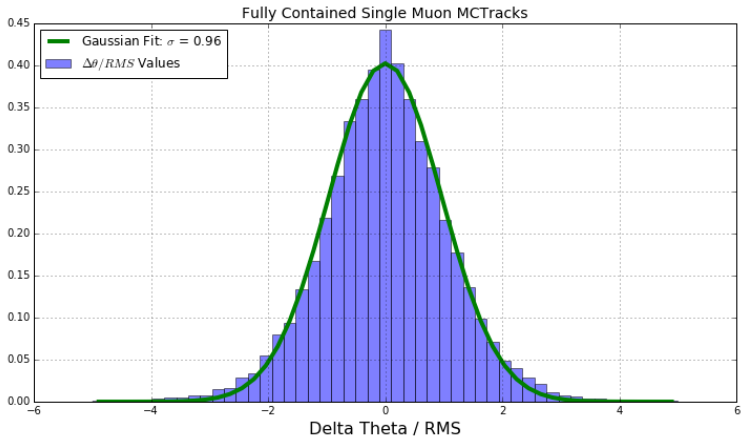

Figure 9: *10 cm segment angular deviations divided by expected Highland RMS for the single muon* MCTrack *sample described in Section 4.3.2.*

5 MCS Performance on Truth-Selected Muons from numuCC Events in Simulation

5.1 Input sample

The input sample to this portion of the analysis is roughly 800,000 MCC7 simulated BNB neutrino interactions without any cosmics simulated. These simulated events are run through a fully automated reconstruction chain and then truth information is used to select muons from numuCC interactions which are eligible for MCS analysis. The SAM definition used for this sample is "prodgenie_bnb_nu_uboone_mcc7_reco2".

5.2 Event selection

The event selection for this subanalysis is truth based. The cuts are:

- There is one neutrino interaction in the event.
- The neutrino interaction is of type numu charged-current, and occurs within the fiducial volume.
- The MCTrack associated with the outgoing muon from the interaction is fully contained within the fiducial volume.
- The MCTrack associated with the outgoing muon from the interaction is at least one meter in length.
- There is a reconstructed track that starts within 3 cm of the start and ends within 3 cm of the end of the aforementioned MCTrack (or vice-versa). This cut is requiring that the track is well reconstructed in terms of position (direction is taken into account later).

After these additional cuts are placed, 13810 events (tracks) remain for MCS analysis.

5.3 MCS Momentum Validation

For this sample of reconstructed tracks, only the 3D trajectory points of each reconstructed track are used as input to the MCS code, described in Section 3. The resulting MCS momentum versus range-based momentum without any cuts other than those described in Section 5.2 can be seen in Figure 10.

In order to compute a bias and a resolution, Figure 10 is sliced in bins of range momentum and a histogram of the fractional momentum difference ($\frac{p_{MCS}-p_{range}}{p_{range}}$) is created for each bin. This distribution is shown for three representative bins in Figure 11. The mean of each distribution is used to compute a bias as function of range momentum, while the standard deviation of each distribution is used to compute a resolution. The bias and resolution for this momentum reconstruction method shown in Figure 12. This figure indicates a positive bias in the MCS momentum resolution on the order of a few percent, with a resolution that decreases from about 11% for contained tracks with true total momentum around 0.5 GeV (which corresponds to a length of about 1.7 meters) to below 8% for contained tracks with true total momentum greater than 0.8 GeV (which corresponds to a length of about 3.1 meters). This agrees reasonably well with the analogous plots created from simulated single muons with MCTracks (Figure 8).

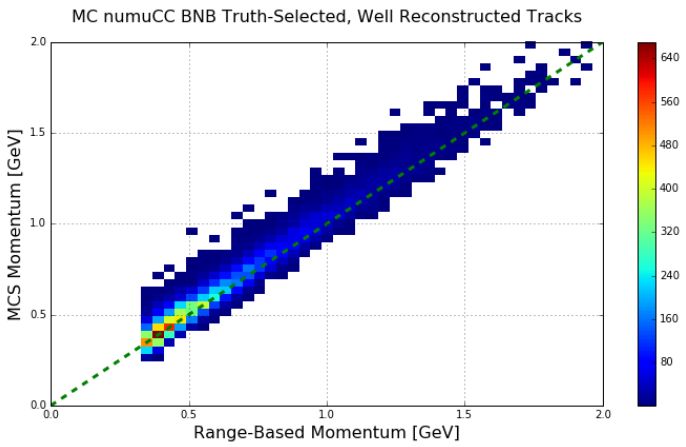

Figure 10: *MCS computed momentum versus range momentum for the truth-selected simulated fully contained, well reconstructed muon tracks from numu charged current events.*

5.4 Highland Validation

For this sample of tracks, the same Highland validation plot is created in exactly the same way as described in Section 4.3.5. For each consecutive pair of segments, the angular scatter in milliradians divided by the Highland expected RMS in millradians is an entry in the histogram shown in Figure 13. From this figure we can see that the Highland formula is valid for well reconstructed tracks in simulation when 10 cm segments are used.

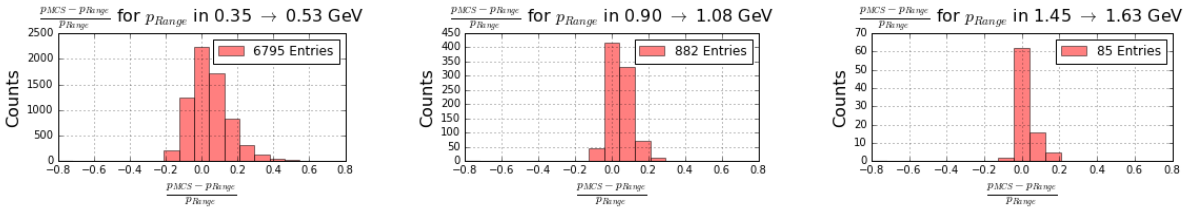

(a) *Fractional momentum difference between 0.35 and 0.53 GeV range momentum.*

(b) *Fractional momentum difference between 0.90 and 1.08 GeV range momentum.*

(c) *Fractional momentum difference between 1.45 and 1.63 GeV range momentum.*

Figure 11: *Fractional momentum difference for a few representative bins of range momentum derived from Figure 10.*

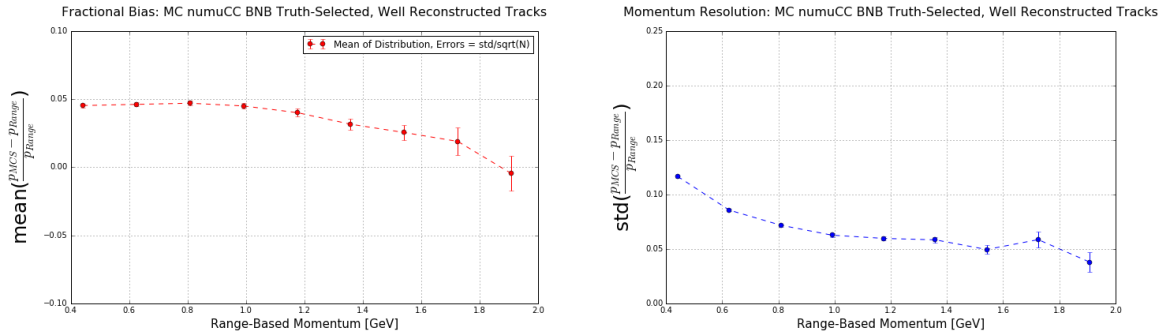

(a) *MCS momentum bias as a function of range momentum.*

(b) *MCS momentum resolution as a function of range momentum.*

Figure 12: *MCS momentum bias and resolution as a function of range momentum for the truth-selected simulated fully contained, well reconstructed muon tracks from numu charged current events.*

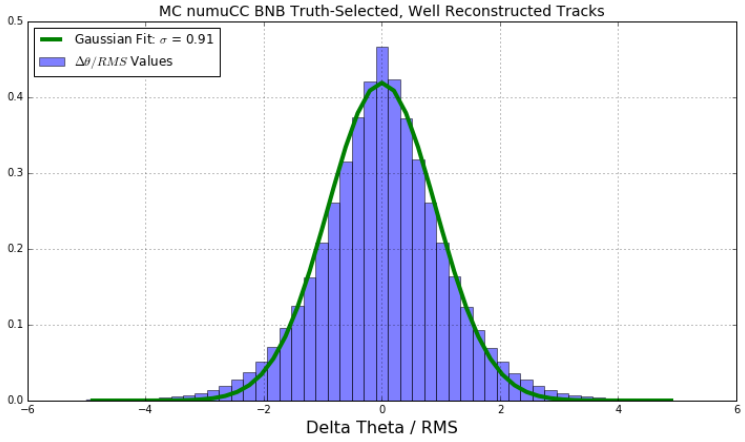

Figure 13: *10 cm segment angular deviations divided by expected Highland RMS for the sample of well reconstructed, neutrino induced muons in simulation.*

5.5 Optimizing Segment Length

One of the tunable parameters in the MCS algorithm is the length of segments into which a track is broken. While shorter segment lengths yield more segments per track and therefore more sampling points to build a stronger likelihood, they also lead to the breakdown of the gaussian nature of scatters. Longer segments tend to have a more gaussian distribution of scatters but lead to fewer sampling points and therefore worse momentum resolution. Additionally, shorter segment lengths tend to have a higher momentum bias. For these reasons there exists an optimal segment length. Figure 14 shows analogous figures to Figure 13 for four different segment lengths ranging between 2 cm and 20 cm, with the same

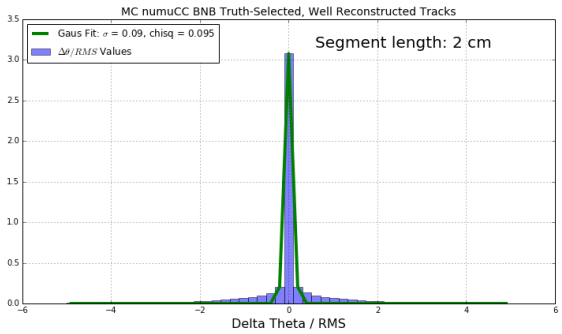

(a) *Highland validation figure for 2 cm segment lengths.*

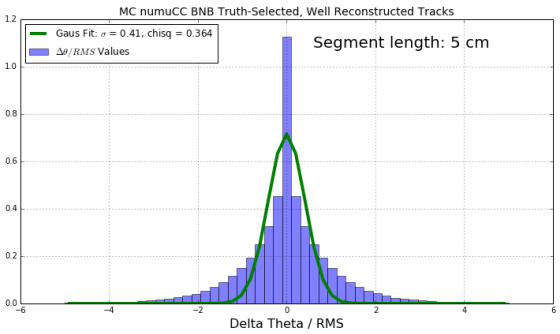

(b) *Highland validation figure for 5 cm segment lengths.*

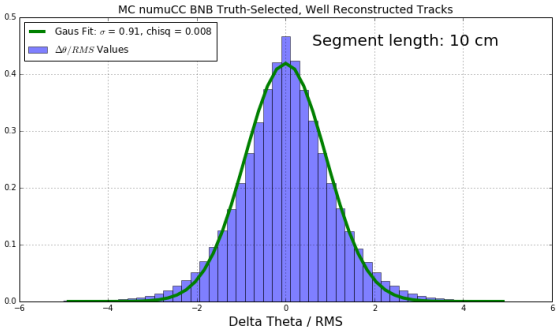

(c) *Highland validation figure for 10 cm segment lengths.*

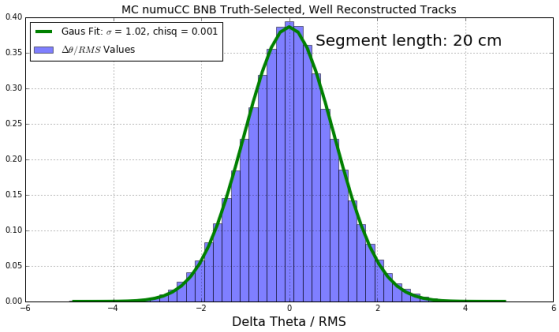

(d) *Highland validation figure for 20 cm segment lengths.*

Figure 14: *Highland validation figures analogous to Figure 13 for various segment lengths, taken from the sample of well reconstructed neutrino-induced truth-selected muons in simulation. The gaussian nature of this plot breaks down for segment lengths that are too short.*

input sample of tracks. From this figure it can be seen that only segment lengths longer than or equal to 10 cm provide truly gaussian distributions.

Figure 15 shows the bias and resolution for the MCS momentum reconstruction method on this same sample. Here we see that shorter segment lengths tend to have a higher bias. Similarly, shorter segment lengths tend to have better resolution but the difference is small at larger range momenta. For range momenta below about 0.5 GeV the difference in resolution between segment lengths grows because the tracks are short enough where the longer segment lengths are not providing enough sampling points for the MCS method to make an accurate estimation of the track momentum. In order to maintain a gaussian distribution of angular scatters while providing enough sampling points for an momentum resolution of below 15% for the shortest viable tracks, a segment length of 10 cm has been chosen for this analysis.

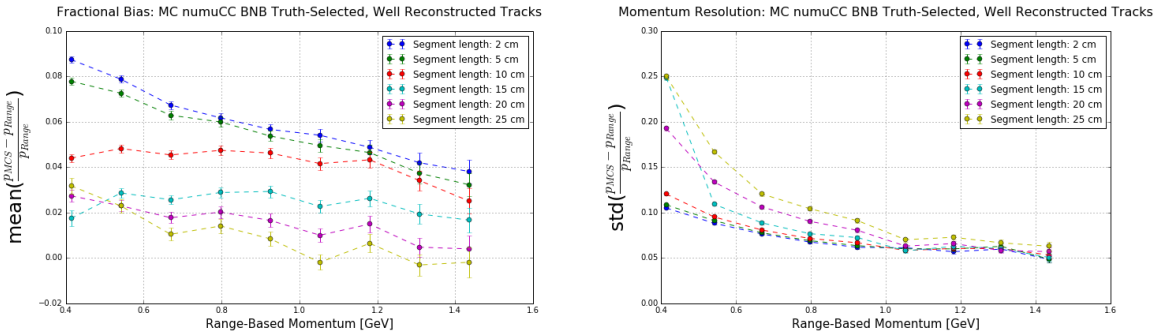

(a) *MCS momentum bias as a function of range momentum for four different segment lengths.*

(b) *MCS momentum resolution as a function of range momentum for four different segment lengths.*

Figure 15: *MCS momentum bias and resolution as a function of range momentum for the selected, well reconstructed neutrino-induced truth-selected muons in simulation.*

5.6 Optimizing Constant Detector Resolution Term

This section describes how the resolution term σ_θ^{res} in the modified Highland equation, Equation 6 is chosen. This constant was chosen *after* choosing the optimal segment length of 10 cm described in Section 5.5. In order to choose a resolution term, a procedure similar to the one described in the segment length optimization section (Section 5.5). This sample of well-reconstructed truth-selected muons from numu charged current interactions in simulation was analyzed with various different resolution terms. It was found that the resolution term has a very small impact for the muons studied in this sample. It is worth noting that this resolution term will have a stronger impact on the energy resolution the higher energy the muons are (as higher energy muons have smaller angular scatters so the resolution term begins to dominate), but since this study only considers contained muons that have lower energy, the term's impact is weak.

The momentum bias and resolution are computed in the usual way for different resolution terms, using the nominal 10 cm segment length in the algorithm. The results can be seen in Figures 16(a) and 16(b) respectively. For 10 cm segments, the resolution terms have small impact on the bias and momentum resolution of the algorithm so long as the resolution parameter isn't exceedingly large (above 5 mrad). Therefore, a default resolution of 2 mrad has been chosen to be used for the entirety of this analysis.

5.7 MCS to Determine Track Direction

This section demonstrates the ability for the multiple coloumb scattering algorithm to determine the direction of a track. The MCS code as it is described in Section 3 works by maximizing a likelihood based on angular scatters between segments of a track along with the expected RMS angular deviation from the modified Highland equation (Equation 6). In practice, there is actually a negative log likelihood that is minimized, meaning the lower the likelihood the more confident the fit is. In order to determine the direction of a track with MCS, one can compute the converged minimum negative log likelihood for the

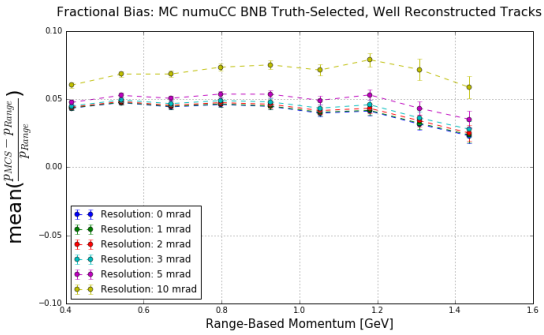

(a) *MCS momentum bias as a function of range momentum for five different resolution terms.*

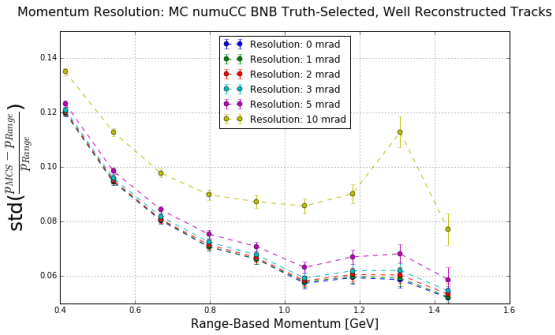

(b) *MCS momentum resolution as a function of range momentum for five different resolution terms.*

Figure 16: *The impact of constant resolution terms, σ_θ^{res} in the modified Highland equation, Equation 6.*

track assuming it is oriented in the correct direction, then reverse the ordering of the trajectory points in the track and compute the converged minimum negative log likelihood for the reversed track. The likelihood should be better (smaller) for tracks in the correct direction than their reversed counterparts.

Given this truth-selected sample in simulation, the true direction of the track is known. The minimized negative log likelihood for each of these tracks both in the correct (forwards) direction and incorrect (backwards) direction can be seen in Figure 17(a). A smaller likelihood here means a better fit in the MCS code. Figure 17(b) shows the difference of these two distributions, forwards minus backwards. Any negative entries in this figure indicate that the forwards-going track had a better fit than backwards-going. This figure shows that MCS can be used as a tool to test track direction.

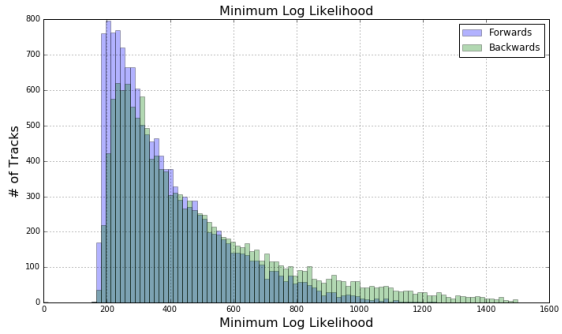

(a) *The minimized negative log likelihood value for each track in the well-reconstructed, fully contained neutrino-induced truth-selected muon tracks in simulation sample, both with tracks oriented in the correct (forwards) direction and reversed (backwards) direction. A smaller likelihood here means a better fit in the MCS code.*

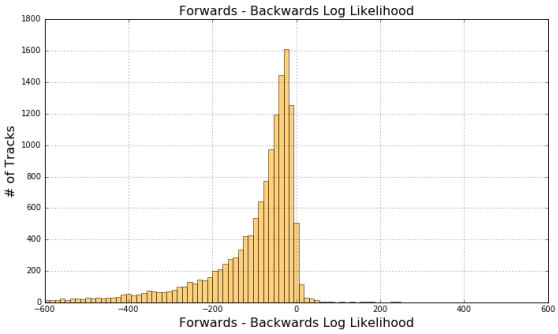

(b) *The difference, forwards minus backwards, of the log likelihoods. Negative entries indicate that the forwards-going tracks had a better fit than the backwards-going ones.*

Figure 17: *Evidence that MCS can be used to determine track directions by analyzing the output of the likelihood fit.*

6 MCS Performance on Automatically Selected Muons from numuCC Events With Cosmics in Simulation

6.1 Input sample

The input sample to this portion of the analysis is roughly 190,000 MCC7 simulated BNB neutrino interactions with CORSIKA cosmics as used by the CCInclusive group and descibed in their interal note[9]. These simulated events are run through a fully automated reconstruction chain and then a fully automated event selection routine described in Section 6.2. The SAM definition used for this sample is "prodgenie_bnb_nu_cosmic_uboone_mcc7_reco2".

6.2 Event selection

The event selection algorithms used are designed to locate ν_μ charged-current interactions, where at least one muon track exits the interaction vertex. The event selection is described in detail in Section 6.2.1 of the MicroBooNE CCInclusive internal note ("Selection IIA: track multiplicity 2 (or larger) and no containment requirement")[9] but the main points will be recapped here. The selection takes as input reconstructed vertices created by the "pmtrack" producer module, reconstructed tracks created by the "pandoraNuPMA" track producer module, and optical hits produced by the "opFlashSat" producer module. The following selection cuts are placed to isolate ν_μ charged-current interactions:

1. The event must have at least one flash inside of the BNB beam-spill window brighter than 50 PE.
2. Two or more reconstructed tracks must originate from the same reconstructed vertex within the fiducial volume (defined in Section 4.2).
3. The tracks must overlap within a 70 cm buffer in the drift (z) direction of the center of the reconstructed optical flash.
4. For events with exactly two tracks originating from the vertex, additional calorimetric-based cuts are applied to mitigate backgrounds from in-time cosmics which produce Michel electrons that get reconstructed as a track.

After these event selection cuts are placed, further cuts are placed to isolate single tracks that are eligible for this MCS analysis.

1. The longest track is assumed to be the muon, and it is the only track studied in this analysis.
2. This track must be at least one meter in length, and it also must match with an MCTrack (Section 4.3.1) originating from the true neutrino interaction in the event. Here, "match" means that the start of the reconstructed track is within 3 cm of the start of the MCTrack, and the end of the reconstructed track is within 3 cm of the end of the MCTrack (or vice-versa).
3. The longest track must be fully contained within the fiducial volume.

After these additional cuts are placed, 1613 events (tracks) remain for MCS analysis. It should be known that there are some inherent pion and proton mis-identification (MID) backgrounds in this sample after these cuts are placed. 88% of the time the identified track is truly a muon. Protons and pions make up the remaining MIDs with 8.6% and 3.4% respectively.

6.3 MCS Momentum Validation

For this sample of reconstructed tracks, only the 3D trajectory points of each reconstructed track are used as input to the MCS code, described in Section 3. The resulting MCS momentum versus range-based momentum without any cuts other than those described in Section 6.2 can be seen in Figure 18. The off-diagonal visible in this figure (where MCS momentum greatly overestimates range momentum) is caused primarily by MIDs, most commonly where the longest track is a proton. Note that there are no "broken tracks" (which is another not-yet-discussed possible explanation for the off-diagonal) because of the track-MCTrack matching requirement described in Section 6.2. Figure 19 divides Figure 18 into those events in which the MCTrack matched to the reconstructed track is a proton, a pion, or a muon. From this figure it is clear comparing MCS momentum to range momentum for contained tracks will provide a handle on separating muon tracks from proton tracks in data (though it is hard to make similar conclusions about pions due to limited statistics in this study).

In order to compute a bias and a resolution, Figure 19(c) is sliced in bins of range momentum and a histogram of the fractional momentum difference ($\frac{p_{MCS}-p_{range}}{p_{range}}$) is created for each bin. This distribution is shown for three representative bins in Figure 20. The mean of each distribution is used to compute a bias a function of range, while the standard deviation of each distribution is used to compute a resolution. The bias and resolution for this momentum reconstruction method is shown in Figure 21. This figure indicates a positive bias in the MCS momentum resolution on the order of a few percent, with a resolution that decreases from about 11% for contained tracks with true total momentum around 0.5 GeV (which corresponds to a length of about 1.7 meters) to below 8% for contained tracks with true total momentum greater than 0.8 GeV (which corresponds to a length of about 3.1 meters). This agrees well with the analogous plots created from simulated single muons with MCTracks (Figure 8).

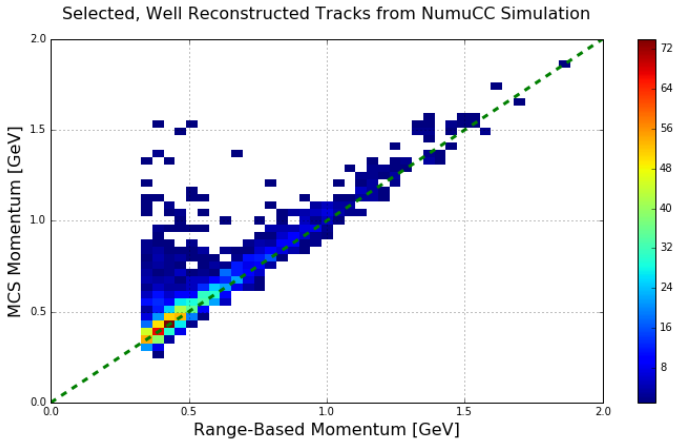

Figure 18: *MCS computed momentum versus range momentum for the automatically selected simulated neutrino-induced fully contained, well reconstructed muon sample without any additional cuts to mitigate MIDs.*

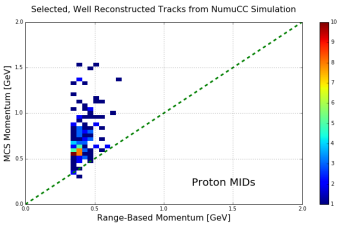

(a) *The subset of events in Figure 18 in which the true identity of the track is a proton.*

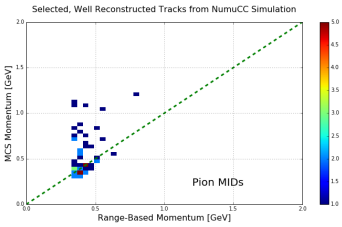

(b) *The subset of events in Figure 18 in which the true identity of the track is a pion.*

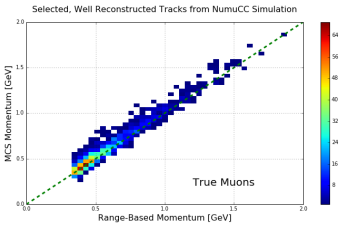

(c) *The subset of events in Figure 18 in which the true identity of the track is a muon.*

Figure 19: *MCS computed momentum versus range momentum for the selected neutrino-induced, well reconstructed fully contained muon sample in simulation broken up by true particle identity of the track.*

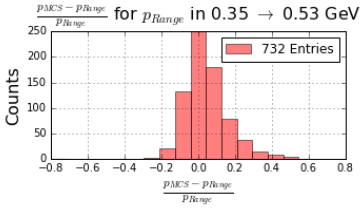

(a) *Fractional momentum difference between 0.35 and 0.53 GeV range momentum.*

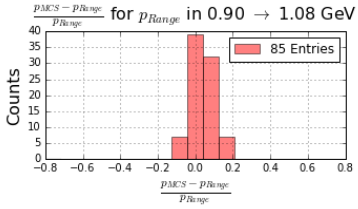

(b) *Fractional momentum difference between 0.90 and 1.08 GeV range momentum.*

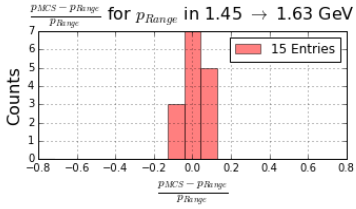

(c) *Fractional momentum difference between 1.45 and 1.63 GeV range momentum.*

Figure 20: *Fractional momentum difference for a few representative bins of range momentum derived from Figure 19(c).*

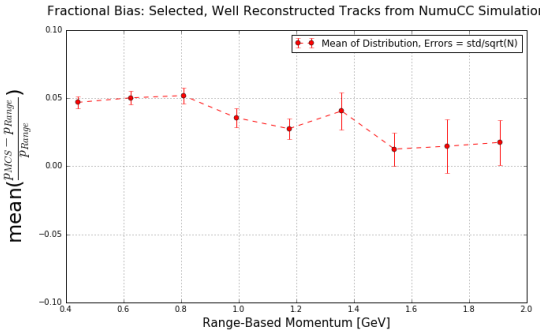

(a) *MCS momentum bias as a function of range momentum.*

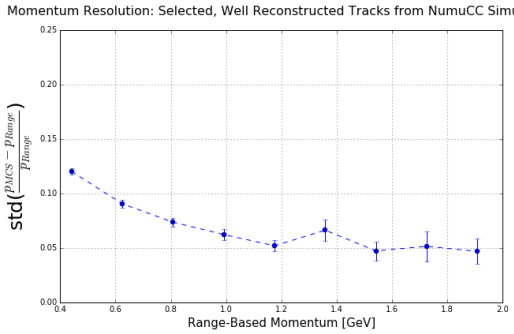

(b) *MCS momentum resolution as a function of range momentum.*

Figure 21: *MCS momentum bias and resolution as a function of range momentum for the selected, well reconstructed neutrino-induced muons in MicroBooNE simulation.*

6.4 Highland Validation

For this sample of contained, automatically selected, well-reconstructed neutrino-induced tracks, the same Highland validation plot is created in exactly the same way as described in Section 4.3.5. For each consecutive pair of segments, the angular scatter in milliradians divided by the Highland expected RMS in millradians is an entry in the histogram shown in Figure 22. From this figure we can see that the Highland formula is valid for automatically selected, well reconstructed neutrino-induced muon tracks in simulation.

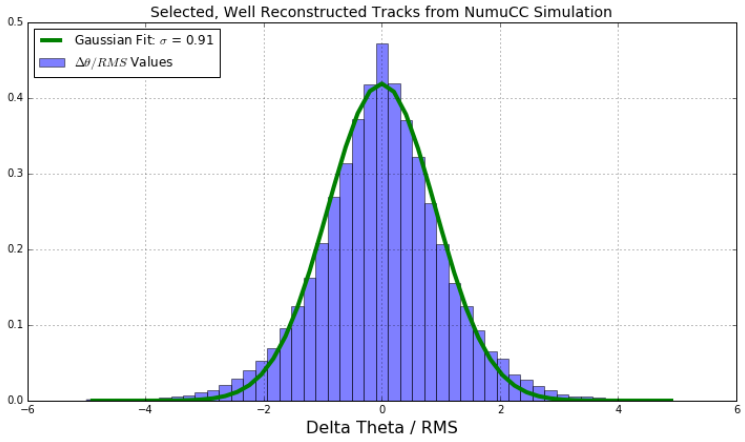

Figure 22: *10 cm segment angular deviations divided by expected Highland RMS for the sample of well reconstructed, neutrino induced muons in simulation.*

7 MCS Performance on Automatically Selected Muons from numuCC Events in MicroBooNE Data

7.1 Input sample

The input sample to this portion of the analysis is roughly 5e19 POT worth of triggered BNB neutrino interactions in MicroBooNE data as used by the CCInclusive group and descibed in their interal note[9]. These events are run through the same fully automated reconstruction chain and event selection routine described in Section 6.1. The SAM definition used for this sample is "prod_bnb_reco_neutrino2016_beamfilter_goodruns_v5".

7.2 Event selection

The exact same event selection cuts are used to identify ν_μ charged-current events in this data sample as described in Section 6.2. The same further cuts to isolate the subset of those events viable for MCS analysis are also placed, with the exception of the cut requiring the reconstructed track matches well with an MCTrack in the event (as there are no MCTracks in real data). In order to accommodate for this difference, a hand scan of the selected events was conducted.

After the event selection cuts, the minimum track length cut, and the containment cuts were placed, 598 events (tracks) remained. Each of these events (tracks) were scanned by hand with an interactive event display. What was shown to the scanner (David Kaleko) were three two-dimensional displays with the raw-wire signals on them. Overlaid on each display was the 2D projection of the 3D reconstructed track and vertex. The scanner looked to ensure the track was well reconstructed (it started within a few cm of the vertex and ended within a few cm of the end of the wire-signal track or vice-versa in all three planes). Additionally the scanner looked for obvious MID topologies like cosmic rays inducing Michel electrons at the reconstructed neutrino vertex (for example when a clear Bragg peak is visible at the neutrino vertex) and also for obvious MID topologies where the track is likely a pion (for example if it charge-exchanges and creates a clear neutral pion decay topology). In general, the scanner chose to be conservative in the sense that if the track didn't look very clearly like a muon from a ν_μ charged-current event, the track (event) was removed from the analysis.

A sample event that was removed by the hand scanner is shown in Figure 23. Only one two-dimensional display is shown (from the collection plane wires), while the 2D projection of the 3D track is shown in black. The 2D projection of the 3D reconstructed neutrino vertex is shown as a small cyan dot near the bottom left of the image. It is clear that the reconstructed track starts in the correct place, but it is truncated and stops before the end of the track. This track was deemed "poorly reconstructed" and was therefore removed from the analysis. A second sample event that was removed by the hand scanner is shown in Figure 24. This event was deemed some form of unknown MID. The reconstructed track matches wire signals well, but this event does not appear to be a clean ν_μ charged-current event, with at least one neutral pion decay visible near the center of the track. A sample event that was deemed acceptable is shown in Figure 25.

7.3 MCS Momentum Validation

For this sample of reconstructed tracks from ν_μ charged current events in data, only the 3D trajectory points of each reconstructed track are used as input to the MCS code, described in Section 3. The re-

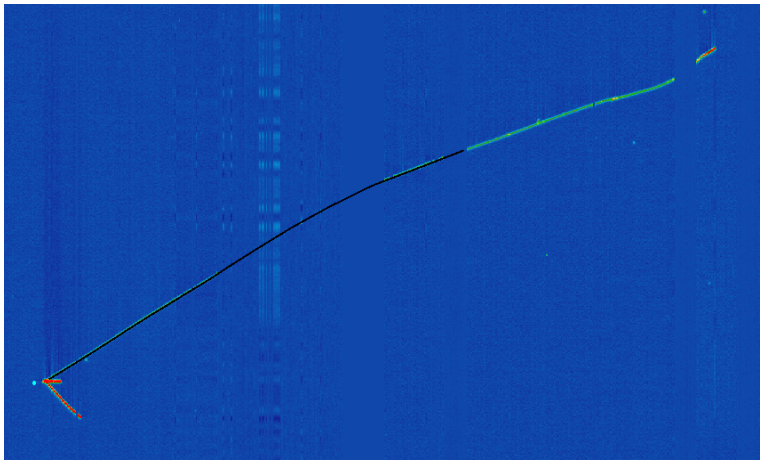

Figure 23: *A hand-scanned data event that was deemed "poorly reconstructed" and removed from this analysis. The 2D projection of the 3D reconstructed track (shown in black overlaid on raw wire signals) clearly stops before it reaches the end of the particle's trajectory.*

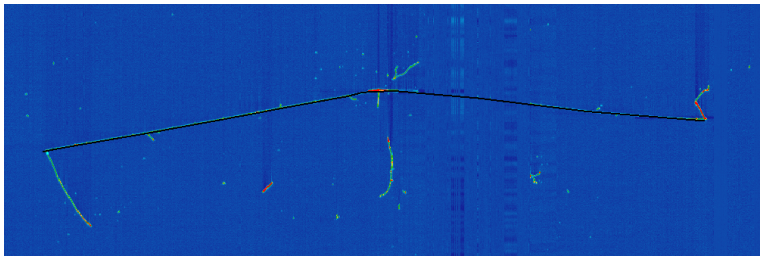

Figure 24: *A hand-scanned data event that was deemed some form of MID and removed from this analysis. The 2D projection of the 3D reconstructed track (shown in black overlaid on raw wire signals) matches raw wire signals well, but this event does not appear to be a clean ν_μ charged-current event, with at least one neutral pion decay visible near the center of the track.*

sulting MCS momentum versus range-based momentum *without any additional hand-scan reconstruction quality checks* can be seen in Figure 26. The off-diagonal visible in this figure (where MCS momentum greatly overestimates range momentum) is caused both by poor track reconstruction (truncated tracks) and MIDs. Figure 27 divides Figure 26 into those events which are handscanned as having poorly reconstructed or obviously MID'd tracks, and those which are well reconstructed. It can be seen that hand-scanning tends to remove the off-diagonal and therefore improve the MCS momentum resolution.

In order to compute a bias and a resolution, Figure 27(b) (the tracks that were hand scanned as being well-reconstructed) is sliced in bins of range momentum and a histogram of the fractional momentum difference ($\frac{p_{MCS}-p_{range}}{p_{range}}$) is created for each bin. This distribution is shown for two representative bins

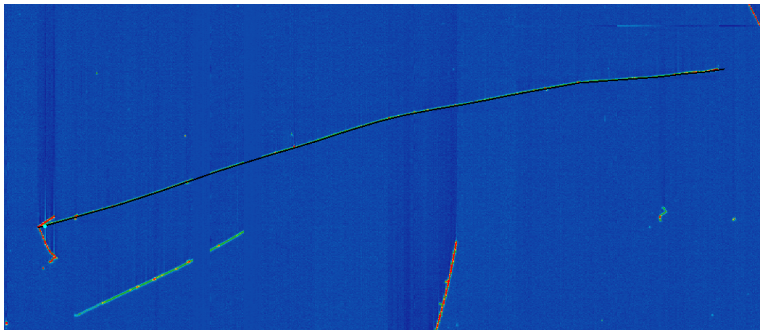

Figure 25: *A hand-scanned data event that was deemed acceptable for MCS analysis. The track looks well reconstructed, and the wire signals indicate that the particle is likely a muon, and a clear Bragg peak can be seen at the end of the track indicating the track is well contained.*

in Figure 28. The mean of each distribution is used to compute a bias as a function of range momentum, while the standard deviation of each distribution is used to compute a resolution. The bias and resolution for this momentum reconstruction method shown in Figure 29. This figure indicates a positive bias in the MCS momentum resolution on the order of a few percent, with a resolution that decreases from about 13% for contained reconstructed tracks with range momentum around 0.5 GeV (which corresponds to a length of about 1.7 meters) to below 8% for contained reconstructed tracks with range momentum greater than 0.8 GeV (which corresponds to a length of about 3.1 meters). This agrees well with the same bias and resolution measurement in simulation as shown in Figure 21. Note the bias and resolution plots stop at a maximum range-based momentum of below 1.4 GeV due to limited statistics.

7.4 Highland Validation

For this sample of contained, selected, well-reconstructed neutrino-induced tracks in MicroBooNE data, the same Highland validation plot is created in exactly the same way as described in Section 4.3.5. For each consecutive pair of segments, the angular scatter in milliradians divided by the Highland expected RMS in millradians is an entry in the histogram shown in Figure 30. From this figure we can see that the Highland formula is valid for well reconstructed, contained muon tracks in data.

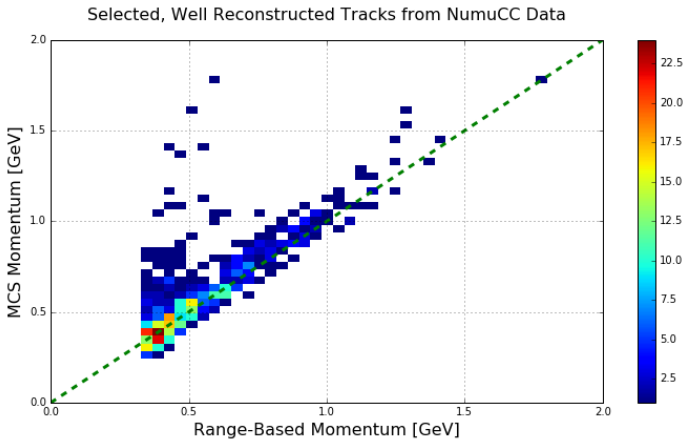

Figure 26: *MCS computed momentum versus range momentum for the selected neutrino-induced fully contained muon sample in data without any additional handscanning to check for reconstruction quality. The off-diagonal where MCS momentum greatly overestimates range momentum is caused by poor track reconstruction (truncated tracks) and MIDs.*

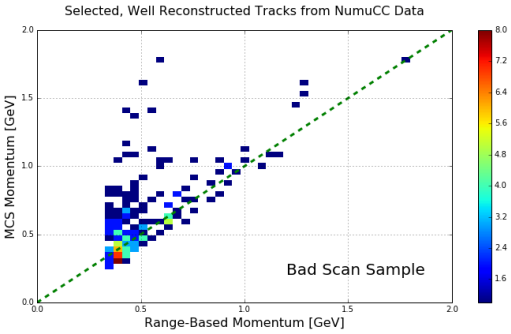

(a) *The subset of events in Figure 26 which were handscanned as having poor reconstruction quality or obvious MID topologies.*

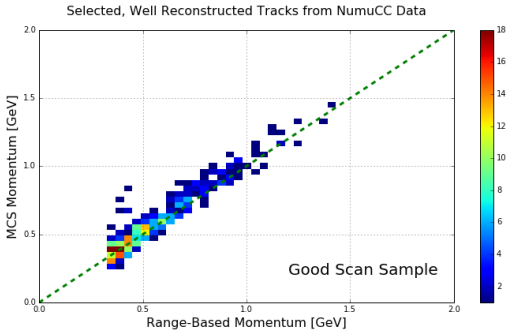

(b) *The subset of events in Figure 26 which were handscanned as having good reconstruction quality or obvious MID topologies.*

Figure 27: *MCS computed momentum versus range momentum for the selected neutrino-induced fully contained muon sample in data hand-scanned as having poorly reconstructed tracks (left) and well reconstructed tracks (right).*

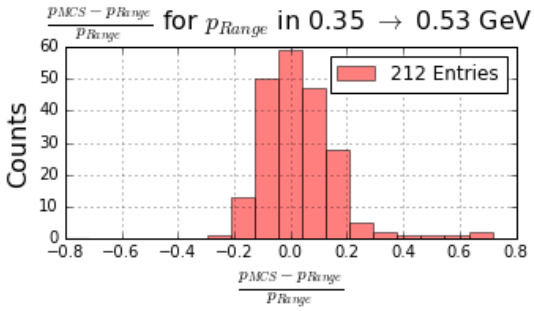

(a) *Fractional momentum difference between 0.35 and 0.53 GeV range momentum.*

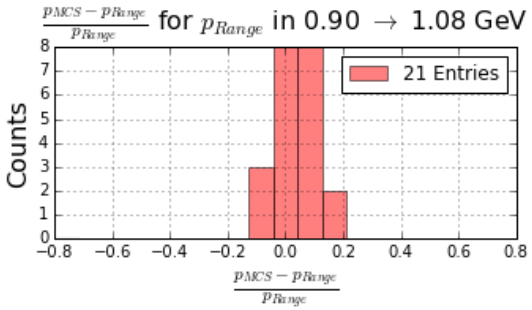

(b) *Fractional momentum difference between 0.90 and 1.08 GeV range momentum.*

Figure 28: *Fractional momentum difference for a few representative bins of range momentum derived from Figure 27(b).*

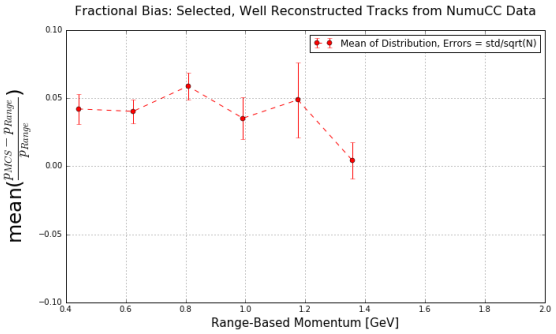

(a) *MCS momentum bias as a function of range momentum.*

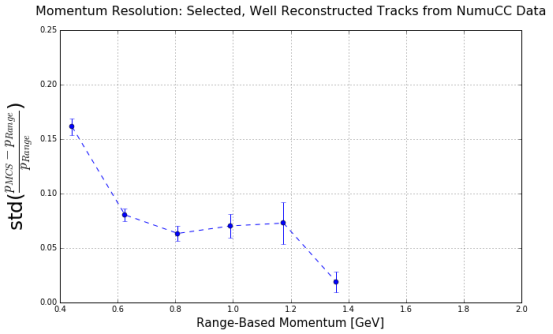

(b) *MCS momentum resolution as a function of range momentum.*

Figure 29: *MCS momentum bias and resolution as a function of range momentum for the selected, well reconstructed neutrino-induced muons in MicroBooNE data.*

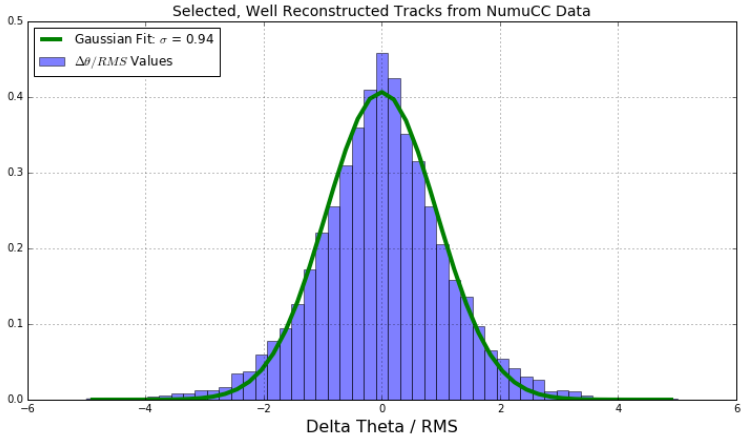

Figure 30: *10 cm segment angular deviations divided by expected Highland RMS for the sample of well reconstructed, neutrino induced muons in MicroBooNE data.*

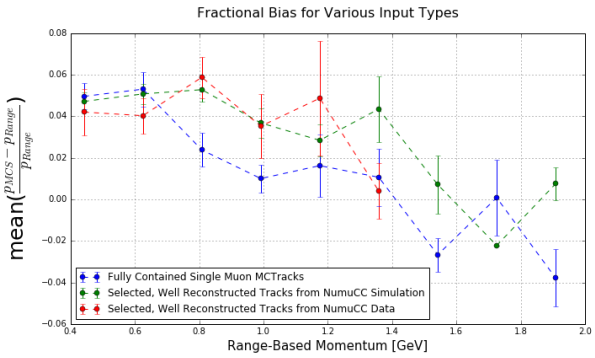

(a) *MCS momentum bias as a function of range momentum.*

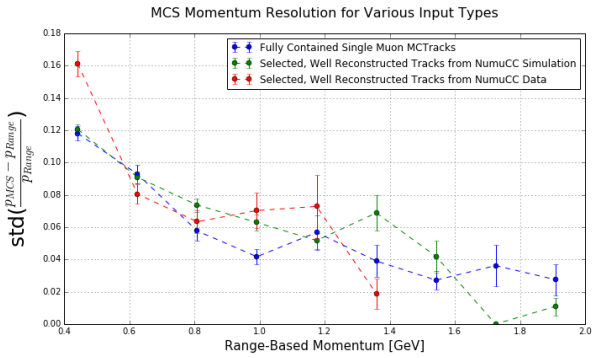

(b) *MCS momentum resolution as a function of range momentum.*

Figure 31: *MCS Momentum resolution for simulated contained single muon* MCTracks *discussed in Section 4.3 (blue), automatically selected contained numuCC-induced muons from simulated BNB+cosmics where the track is well-reconstructed and matches with the true muon track discussed in Section 6 (green), and automatically selected contained numuCC-induced muons from MicroBooNE data where the track is deemed well-reconstructed and likely-muon from hand scanning discussed in Section 7.*

8 Conclusions

This note has discussed the multiple coloumb scattering technique for estimating the momentum of a three dimensional reconstructed track and provided motivation for demonstration of the capabilities of this tool within the neutrino LArTPC community. The details of the implementation of this code have been described. The gaussian nature of scatters predicted by the Highland formula has been demonstrated. Additionally the performance of this method has been quantified in three different forms of simulation of fully contained tracks (single muon MCTracks, truth-selected simulated BNB neutrino events, and automatically-selected selected BNB + cosmic neutrino events) as well as in approximately 0.5e20 POT of MicroBooNE data. The methods used to optimize the segment length (10 cm) and detector resolution term (2 mrad) in the MCS algorithm have been described. To summarize the performance on these different fully contained track samples, the bias and resolution for the different samples are overlaid in Figure 31. Other uses besides momentum reconstruction for the MCS technique have been described, including using it as a tool for identification of poorly reconstructed tracks, determination of track direction, particle identification.

9 Possible Plots for Publication

Here are a few plots that I think should be considered for the publication. Bear in mind, in my opinion the publication should have its scope kept small so as to get it published in a very quick time scale. These plots of course can be modified, their captions changed, etc... I am just putting them here to paint a picture for the readers of this technote what I think should be included in the publication.

1. Figure 32 is a general image whose purpose is to aid the reader in understanding what MCS is and

how the code works. I'm not sure this one is public-domain, but I can easily make my own version of it if necessary.

2. Figure 33 is an image whose purpose is to validate using range-based momentum in place of true-momentum when the analysis is done on real data where true-momentum obviously is unknown.
3. Figure 34 is an image showing the MCS momentum versus range momentum for the automatically selected, handscanned data events.
4. Figure 35 is an overlay of MCS momentum bias and resolution for various different types of inputs (MCTracks in MC, reconstructed tracks in MC, reconstructed tracks in data). I'll note that since MCTracks are sort of MicroBooNE specific, it is possible (and probably best) to leave them out of the publication entirely and therefore avoid having to describe them to readers.

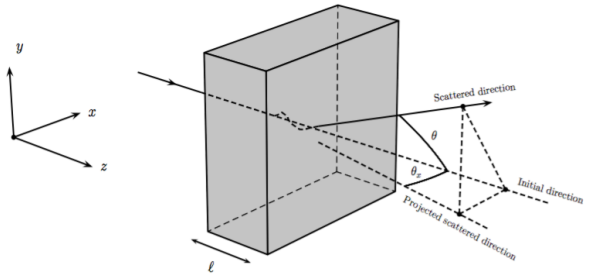

Figure 32: *The particle's trajectory is deflected as it traverses through the material [6].*

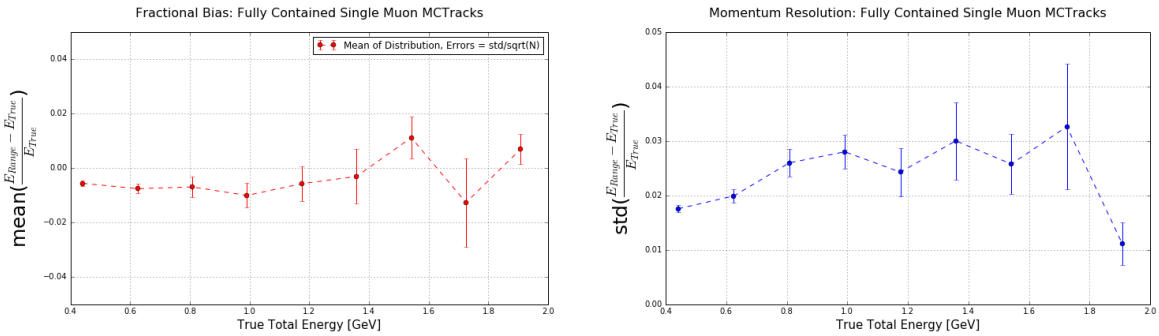

(a) *Range energy bias as a function of true energy.* (b) *Range energy resolution as a function of true energy.*

Figure 33: *Range energy and true energy bias and resolution for the single muon* MCTrack *sample described in Section 4.3.2.*

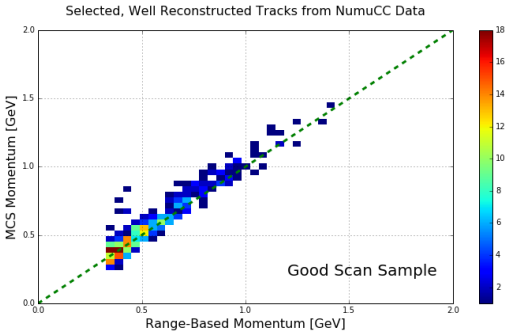

Figure 34: *MCS computed momentum versus range momentum for the selected neutrino-induced fully contained muon sample in data hand-scanned as having well reconstructed, likely-muon tracks.*

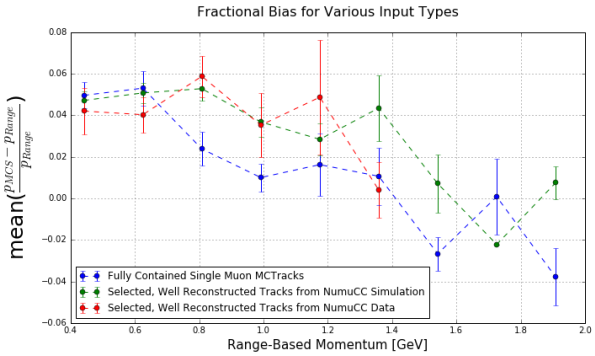

(a) *MCS energy bias as a function of range energy.*

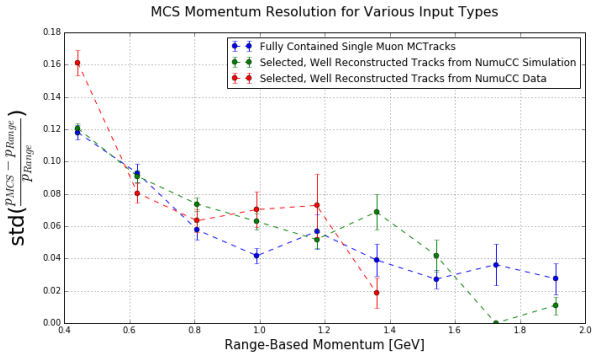

(b) *MCS energy resolution as a function of range energy.*

Figure 35: *MCS Momentum resolution for simulated contained single muon* MCTracks *discussed in Section 4.3 (blue), automatically selected contained numuCC-induced muons from simulated BNB+cosmics where the track is well-reconstructed and matches with the true muon track discussed in Section 6 (green), and automatically selected contained numuCC-induced muons from MicroBooNE data where the track is deemed well-reconstructed and likely-muon from hand scanning discussed in Section 7.*

References

[1] Table 289: Muons in Liquid argon (Ar) http://pdg.lbl.gov/2012/AtomicNuclearProperties/MUON_ELOSS_TABLES/muonloss_289.pdf

[2] J. S. Marshall and M. A. Thomson, Eur. Phys. J. C **75**, no. 9, 439 (2015) doi:10.1140/epjc/s10052-015-3659-3 [arXiv:1506.05348 [physics.data-an]].

[3] D. E. Groom, N. V. Mokhov and S. Striganov, "Muon Stopping Power and Range Tables: 10 MeV - 100 TeV" Table 5 http://pdg.lbl.gov/2012/AtomicNuclearProperties/adndt.pdf

[4] A. A. Aguilar-Arevalo *et al.* [MiniBooNE Collaboration], Improved Search for $\bar{\nu}_\mu \to \bar{\nu}_e$ Oscillations in the MiniBooNE Experiment, Phys. Rev. Lett. **110**, 161801 (2013). doi:10.1103/PhysRevLett.110.161801 [arXiv:1207.4809 [hep-ex], arXiv:1303.2588 [hep-ex]].

[5] S. Lockwitz, The MicroBooNE LArTPC, http://www-microboone.fnal.gov/talks/dpfMicroBooNELArTPC.pdf.

[6] L. Kalousis, Momentum measurement via Multiple Coulomb Scattering with the MicroBooNE detector, MicroBooNE Doc-DB-3733.

[7] V. L. Highland, Some Practical Remarks on Multiple Scattering, Nucl. Instrum. Methods **129** (1975) 104-120.

[8] L. Kalousis, Muon momentum measurement via Multiple Coulomb Scattering in argon, MicroBooNE Doc-DB-4050.

[9] An et al, Selection of charged-current ν_μ inclusive events - Internal Note, MicroBooNE Doc-DB-5851 http://microboone-docdb.fnal.gov:8080/cgi-bin/RetrieveFile?docid=5851&filename=cc-incl-neutrino2016-v2.7.pdf&version=9